Supplementary Data

Soluble Antigen Arrays Efficiently Deliver Peptides and Arrest Spontaneous Autoimmune Diabetes

Rebuma Firdessa-Fite, Stephanie N. Johnson, Martin A. Leon, Mohsen Khosravi-Maharlooei, Rocky L. Baker, Joshua O. Sestak, Cory Berkland, Remi J. Creusot

Table S1. **List of antibodies used to analyze major APC populations for SAgA uptake studies**. All antibodies are anti-mouse and purchased from Biolegend.

Target	Clone	Conjugate	Dilution	RRID
CD8a	53-6.7	APC/Cy7	1:400	AB_312753
CD11b	M1/70	APC	1:400	AB_312795
CD11c	N418	PE	1:300	AB_313777
CD45	30-F11	BV510	1:400	AB_2563061
CD45R/B220	RA3-6B2	BV421	1:400	AB_10933424
F4/80	BM8	PE/Cy7	1:300	AB_893478

Table S2. **List of antibodies used to characterize T cell responses to peptides and SAgAs**. All antibodies are anti-mouse and purchased from Biolegend, except for Foxp3 (ThermoFisher).

Target	Clone	Conjugate	Dilution	RRID
CD4	GK1.5	BV421	1:400	AB_10900241
CD8a	53-6.7	APC/Cy7	1:400	AB_312753
CD25 (IL-2Ra)	PC61	APC	1:400	AB_312861
CD44	IM7	AF700	1:400	AB_493713
CD45.1	A20	PE/Cy7	1:300	AB_1134168
CD45.2	104	APC	1:400	AB_389211
CD73	TY/11.8	FITC	1:400	AB_2716076
CD223 (Lag-3)	C9B7W	PE	1:300	AB_2133343
CD279 (PD-1)	RMP1-30	PE/Cy7	1:300	AB_572017
Foxp3	FKJ-16s	PerCP/Cy5.5	1:100	AB_914351
FR4	12A5	PE	1:400	AB_1134202
IFN-γ	XMG1.2	FITC	1:100	AB_315400
IL-10	JES5-16E3	APC	1:100	AB_315364
KLRG1 (MAFA)	2F1/KLRG1	APC/Cy7	1:400	AB_2566554

Table S3. **List of MHC tetramers used to identify endogenous antigen-specific T cells**. All tetramers were produced by the NIH Tetramer Core Facility and validated at Columbia University (p79, Ins, GAD65) or the University of Colorado Denver (2.5HIP).

Tetramer	MHC/peptide	Conjugate	Dilution
p79-Tetramer	I-A(g7)/ AAAAVRPLWVRMEAA	PE	1:400
2.5HIP-Tetramer	I-A(g7)/ LQTLALWSRMD	APC	1:200
Ins-Tetramer	I-A(g7)/ HLVERLYLVCGEEG	PE	1:400
GAD65-Tetramer	I-A(g7)/ KKGAAALGIGTDSVI	BV421	1:400

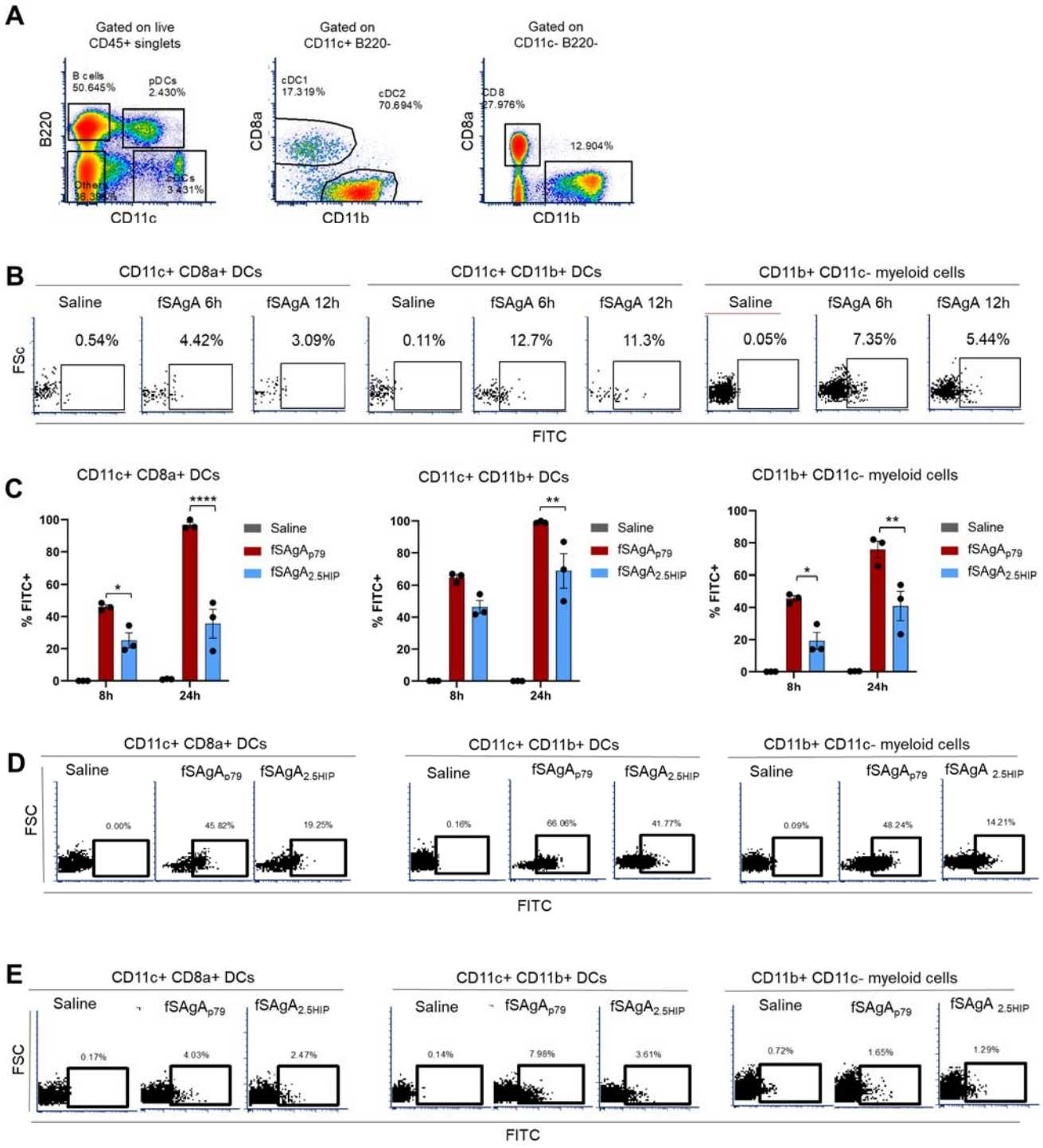

Figure S1. **Uptake of SAgA by different immune cells**. (**A**) Gating strategy for immune cell populations analyzed for SAgA uptake in vitro and in vivo (data shown are from spleen). (**B**) Representative dot plots of fSAgA uptake by CD11c+ CD8a+ resident dendritic cells (cDC1), CD11c+ CD11b+ migratory dendritic cells (cDC2) and CD11b+ CD11c- myeloid cells after injection of 5nmol of fSAgA$_{mix}$ (equimolar mix of fSAgA$_{p79}$ and fSAgA$_{2.5HIP}$) via s.c. in the neck fold. (**C-E**) Relative uptake of fSAgA$_{p79}$ vs fSAgA$_{2.5HIP}$ by cDC1, cDC2 and other myeloid cells at 8h and 24h time points presented as bar graph (**C**) and representative dot plots from 8h time point (**D**) in vitro and 6h after s.c. injection of 5nmol fSAgA$_{p79}$ or fSAgA$_{2.5HIP}$ at the neck fold in vivo (**E**). In panel C, bar graphs show the show the mean ± SEM from 3 biological replicates (mice) per group. Statistical analysis was performed using two-way ANOVA/Tukey.

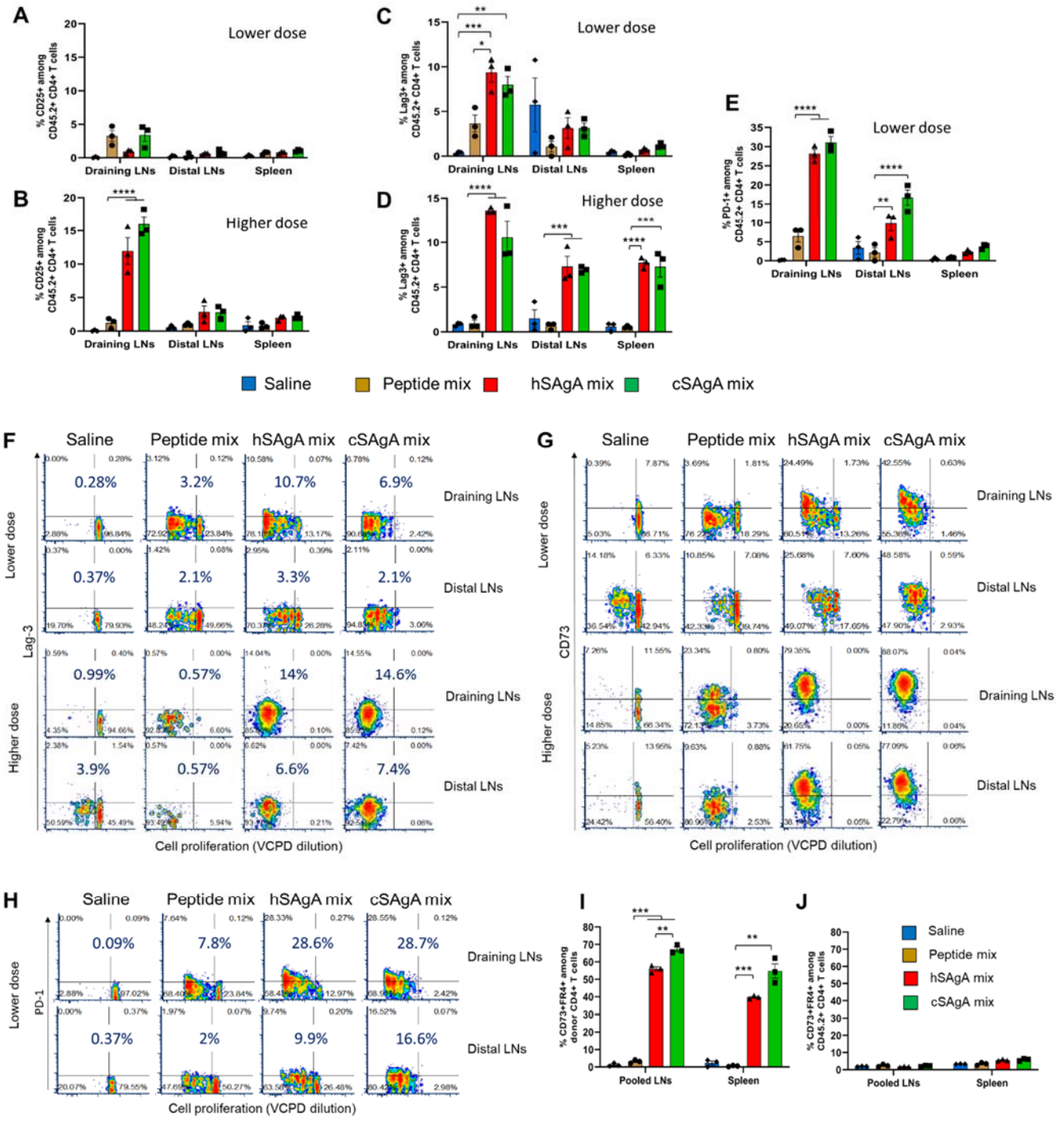

Figure S2. Response of adoptively transferred BDC2.5 CD4+ T cells to a single treatment at lower dose (1 nmol peptides; 0.1 nmol SAgAs; panels A,C,E) or higher dose (5 nmol peptides; 0.5 nmol SAgAs; panels B,D,I,J). The dose given is for each peptide (p79 and 2.5HIP) in the mix. Responses were measured by flow cytometry 3 days after a single treatment, gating on donor CD45.2+ CD4+ T cells and consisted of: % CD25+ at lower (**A**) and higher doses (**B**), % Lag-3+ at lower (**C**) and higher doses (**D**), % PD-1+ (**E**; only measured in lower dose group). Draining LNs were axillary, brachial and cervical; distal LNs were mesenteric and pancreatic, pooled LNs had all of them. Higher background response to saline in distal LNs is attributed to recognition of endogenous antigens by BDC2.5 T cells in PLNs. (**F-H**) Representative density plots are provided for Lag-3 (F), CD73 (G) and PD-1 (H), shown as a function of cell division. (**I,J**) Percentage of CD73+ FR4+ cells in high dose group gated on donor (CD45.2+) CD4+T cells (I) and recipient (CD45.1+) T cells (J). In recipient (CD45.1+) CD4+ T cells, the percentage of CD25+ was 5-7%, and that of Lag-3+ was <1% across all groups. The percentage of PD-1+ in recipient CD4+ T cells was <1% in LNs and 1.5-2% in spleen in all four groups. Bars represent the mean ± SEM from 3 mice/group. Statistical analysis was performed using two-way ANOVA/Tukey for all panels.

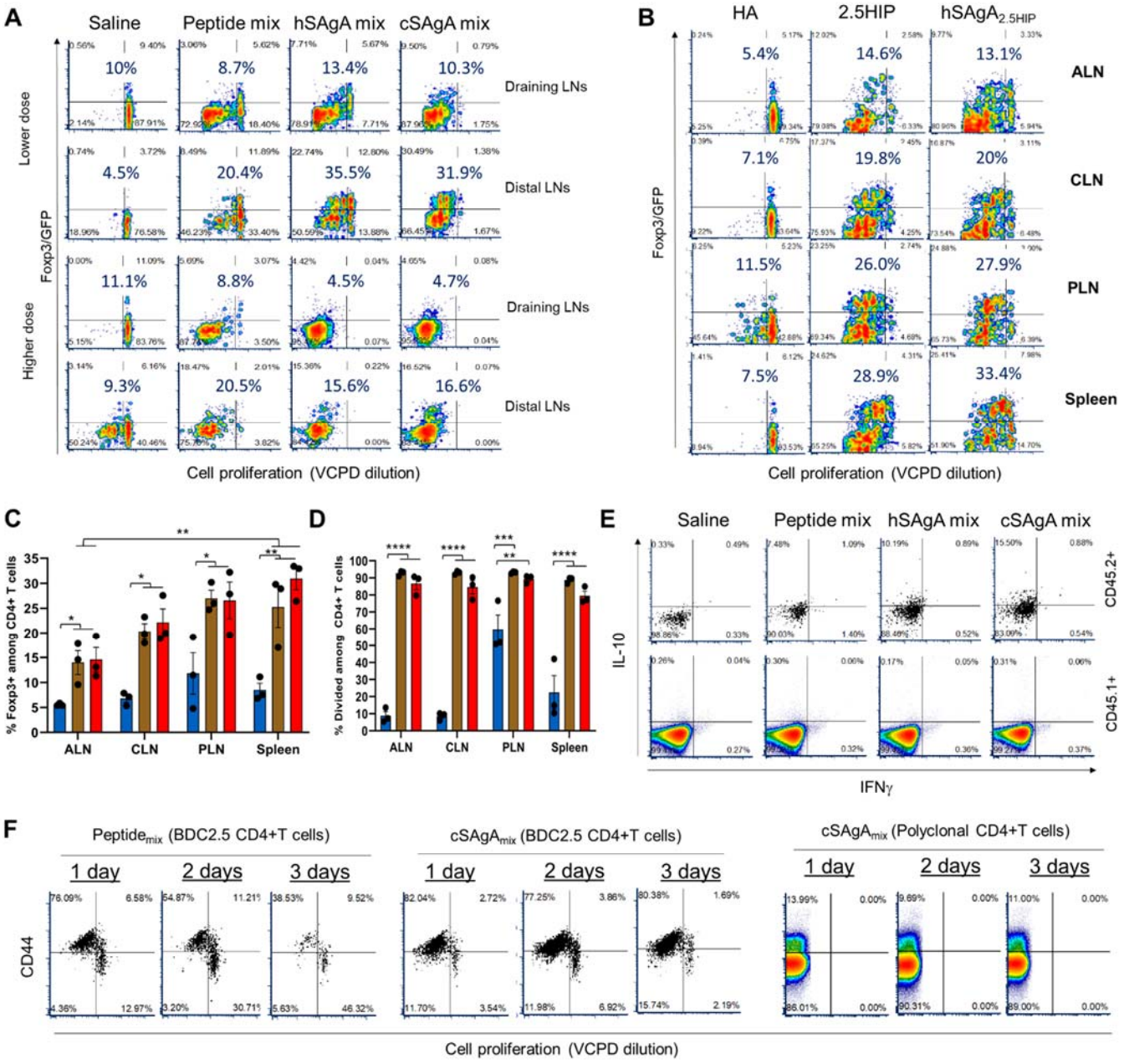

Figure S3. Regulatory responses of adoptively transferred BDC2.5 CD4+ T cells to SAgAs or peptides. (**A**) Representative density plots of Foxp3 expression versus proliferation of BDC2.5 CD4+ T cells with Foxp3/GFP reporter in response to a single treatment at lower dose (1 nmol peptides; 0.1 nmol SAgAs) or higher dose (5 nmol peptides; 0.5 nmol SAgAs). The dose given is for each peptide (p79 and 2.5HIP) in the mix. Responses were measured by flow cytometry 3 days after treatment, gating on CD45.2+ CD4+ T cells. Draining LNs were axillary, brachial and cervical; distal LNs were mesenteric and pancreatic. (**B,C,D**). Foxp3 expression and proliferation in response to a single treatment with 2.5HIP alone as hSAgA (0.2 nmol) or free peptide (2 nmol), measured by flow cytometry 4 days after treatment. Data shown are representative density plots (B) and bar graphs showing the percentage of Foxp3+ (C) and divided cells (D), gated on donor CD45.2+ CD4+ T cells (mean ± SEM, n=3/group). Statistical analysis was performed using two-way ANOVA/Tukey. ALN, CLN and PLN are axillary, cervical and pancreatic LNs respectively. Higher background response to control treatment (saline or HA) in distal LNs is due to recognition of endogenous antigens by BDC2.5 T cells in PLNs. (**E**) Representative dot plots and density plots showing the expression of IL-10 and IFNγ in donor CD45.2+ T cells and recipient CD45.1+ T cells as control, all gated on CD4+ T cells and same conditions as in (A). (**F**) Representative dot plots showing persistence of antigen presentation to transferred BDC2.5 CD4+ T cell responses in vivo following a single injection of 0.5 nmol $cSAgA_{mix}$ or 5nmol of free peptide mix (recipient CD45.1+ CD4+ T cells shown as control).

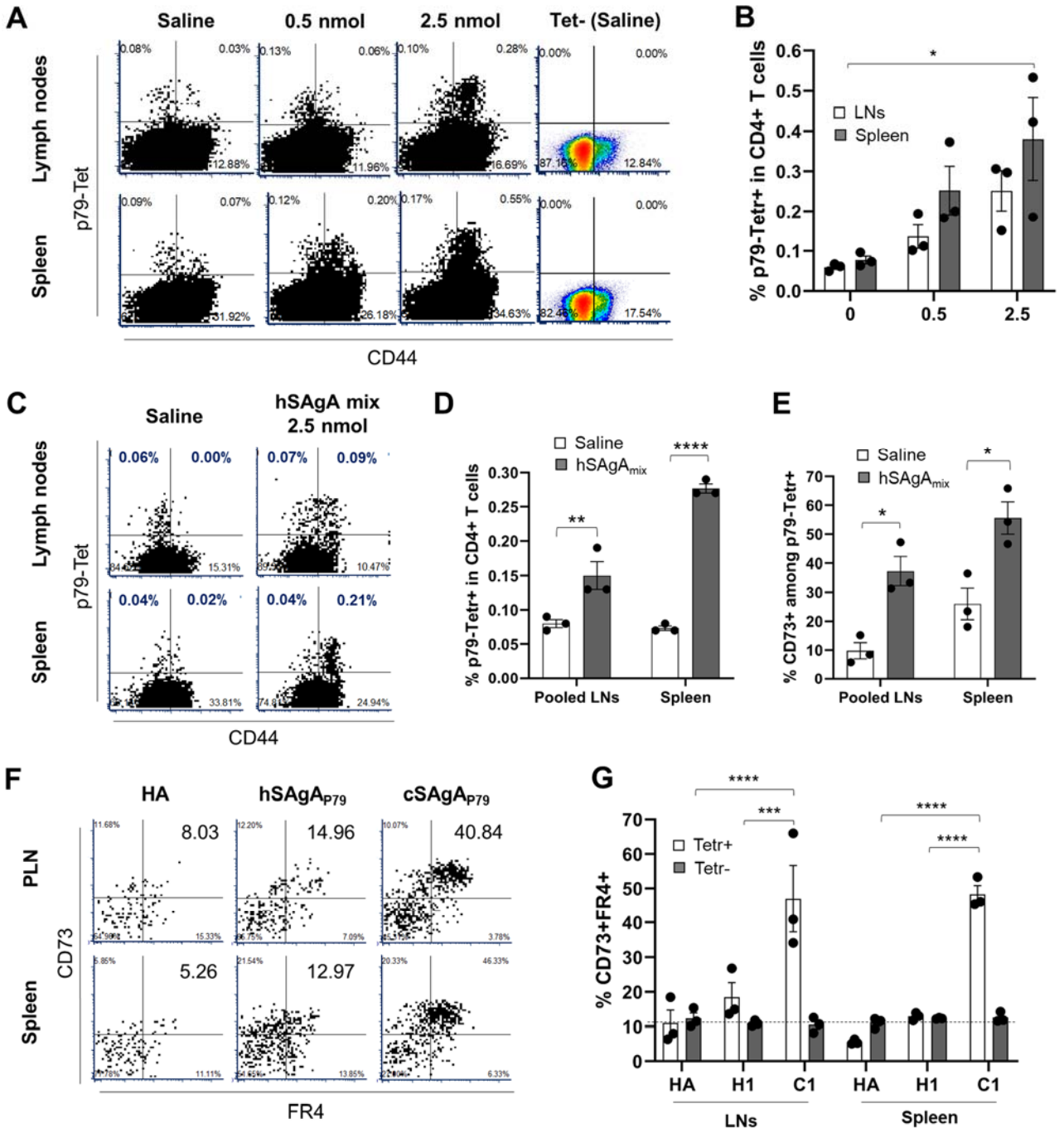

Figure S4. Phenotype of p79-reactive CD4+ T cells after different treatment periods. (**A**) Detection of p79-Tetr+ T cells and their CD44 expression among CD4+ T cells following 6 weekly doses of hSAgA$_{mix}$ (0.5 or 2.5nmol each), analyzed 3 days after the last dose by flow cytometry. (**B**) Clonal expansion of p79-Tetr+ (gated on CD4+ T cells) summarizing representative data shown in (A). (**C-E**) Persistence of p79-Tetr+ T cells following weekly treatments with hSAgA$_{mix}$ (2.5nmol) from 8 to 15 weeks of age, then interrupted for 21 weeks until 36 weeks of age when analysis was performed by flow cytometry. Representative data on detection of p79-Tetr+ and their CD44 expression among CD4+ T cells (C), with bar graphs summarizing the frequency of p79-Tetr+ cells among CD4+ T cells (D) and CD73+ among p79-Tetr+ CD4+ T cells (E). (**F**) Expression of CD73 and FR4 on p79-Tetr+ T cells following 2 doses of SAgA (2.5nmol), two days apart, analyzed 3 days after the last dose by flow cytometry. (**G**) Percentage of CD73+ FR4+ cells among p79-Tetr+ CD4+ T cells and Tetr- CD4+ T cells. All bar graphs show mean ± SEM (n=3/group). Statistical analysis was performed using two-way ANOVA/Tukey for all bar graphs. HA: HA alone; H1: hSAgA$_{p79}$; C1: cSAgA$_{p79}$.

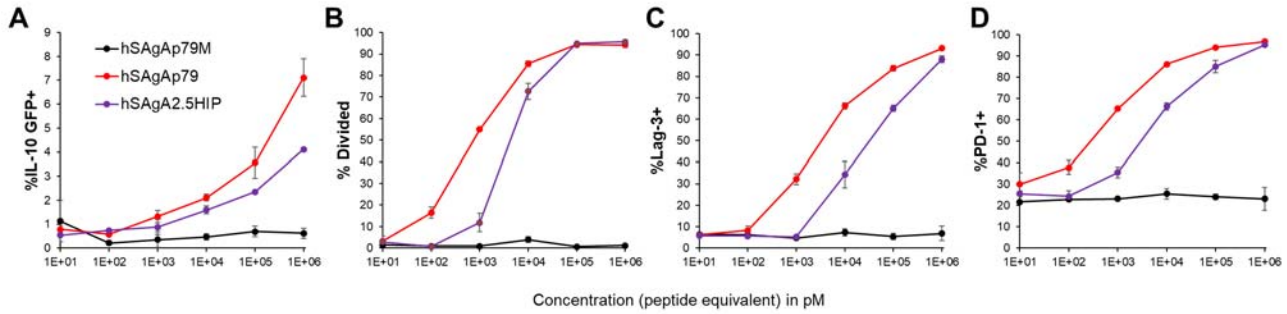

Figure S5. In vitro antigen-specific T cell responses to p79 and 2.5HIP on SAgA. Splenocytes (90% from NOD mice and 10% from congenic BDC2.5 mice) were cultured in the presence of titrated concentrations of $hSAgA_{p79}$ or $hSAgA_{2.5HIP}$. hSAgA with p79M (with permuted mutant of p79 to which BDC2.5 are non-responsive) was used as control. The BDC2.5 T cells carried the IL-10/GFP reporter (ref.9) and were labeled with Violet Cell Proliferation Dye prior to culture. Three days later, the % of IL-10/GFP (**A**), % divided (proliferation dye dilution) (**B**), % Lag-3+ (**C**) and PD-1+ (**D**) was measured on congenic antigen-specific BDC2.5 T cells.

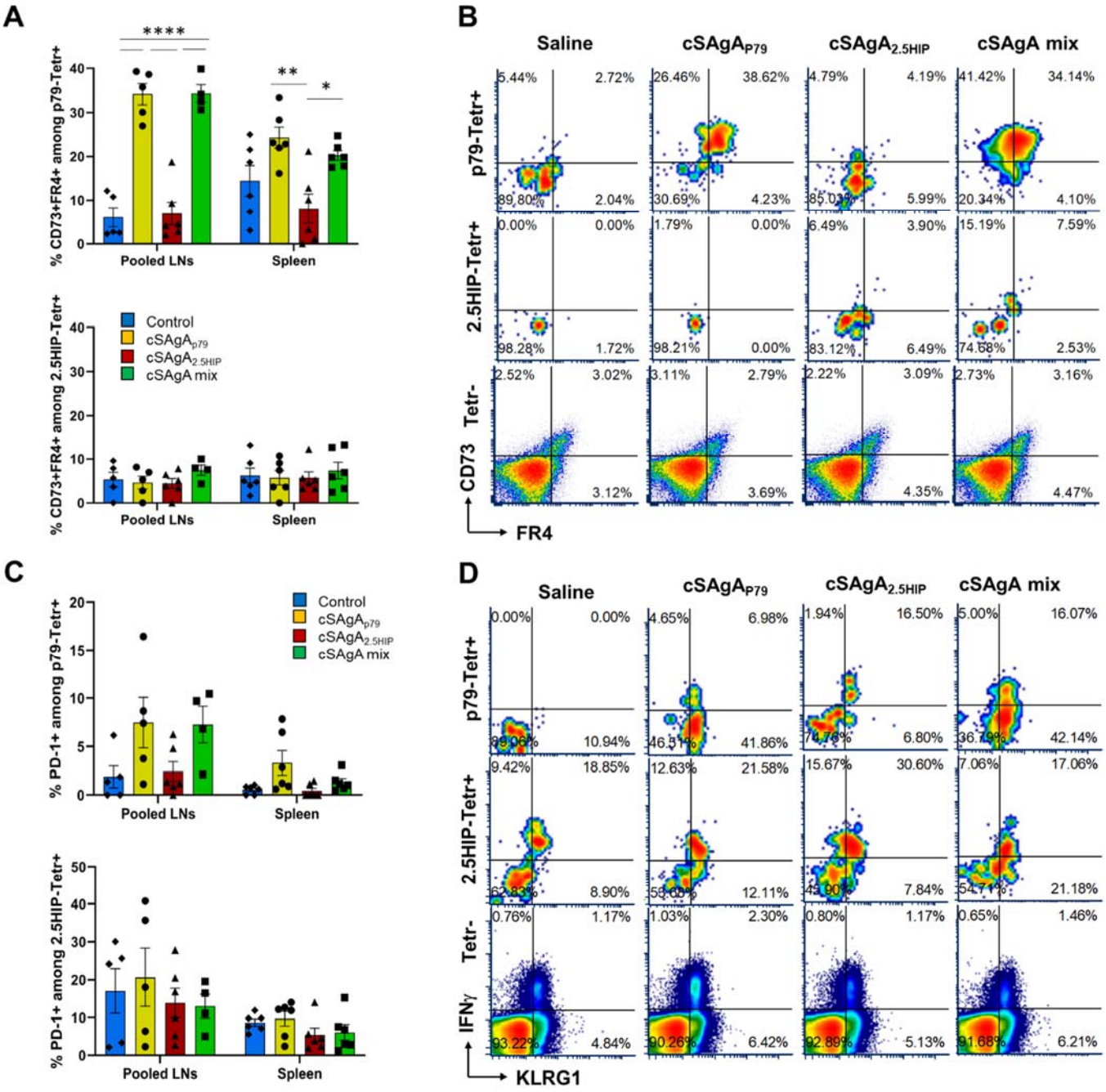

Figure S6. Responses of endogenous p79 and 2.5HIP-reactive CD4+ T cells to single or mixed cSAgAs. (**A**,**B**) Expression of CD73 and FR4 on p79-Tetr+ and 2.5HIP-Tetr+ CD4+ T cells, showing % of CD73+ FR4+ among Tetr+ cells from pooled LNs and spleen in bar graphs (A) and representative dot plots from pooled LNs as example, including Tetr- cells as gating control (B). (**C**) Expression of PD-1 on p79-Tetr+ and 2.5HIP-Tetr+ CD4+ T cells, showing % of PD-1+ among Tetr+ cells from pooled LNs and spleen in bar graphs. (**D**) Expression KLRG1 and IFNγ on p79-Tetr+, 2.5HIP-Tetr+ and Tetr- CD4+ T cells, showing representative density plots from spleen as example. All graphs (A,C) show the mean ± SEM of 4-6 mice per group. Statistical analysis was performed using two-way ANOVA/Tukey for all bar graphs.

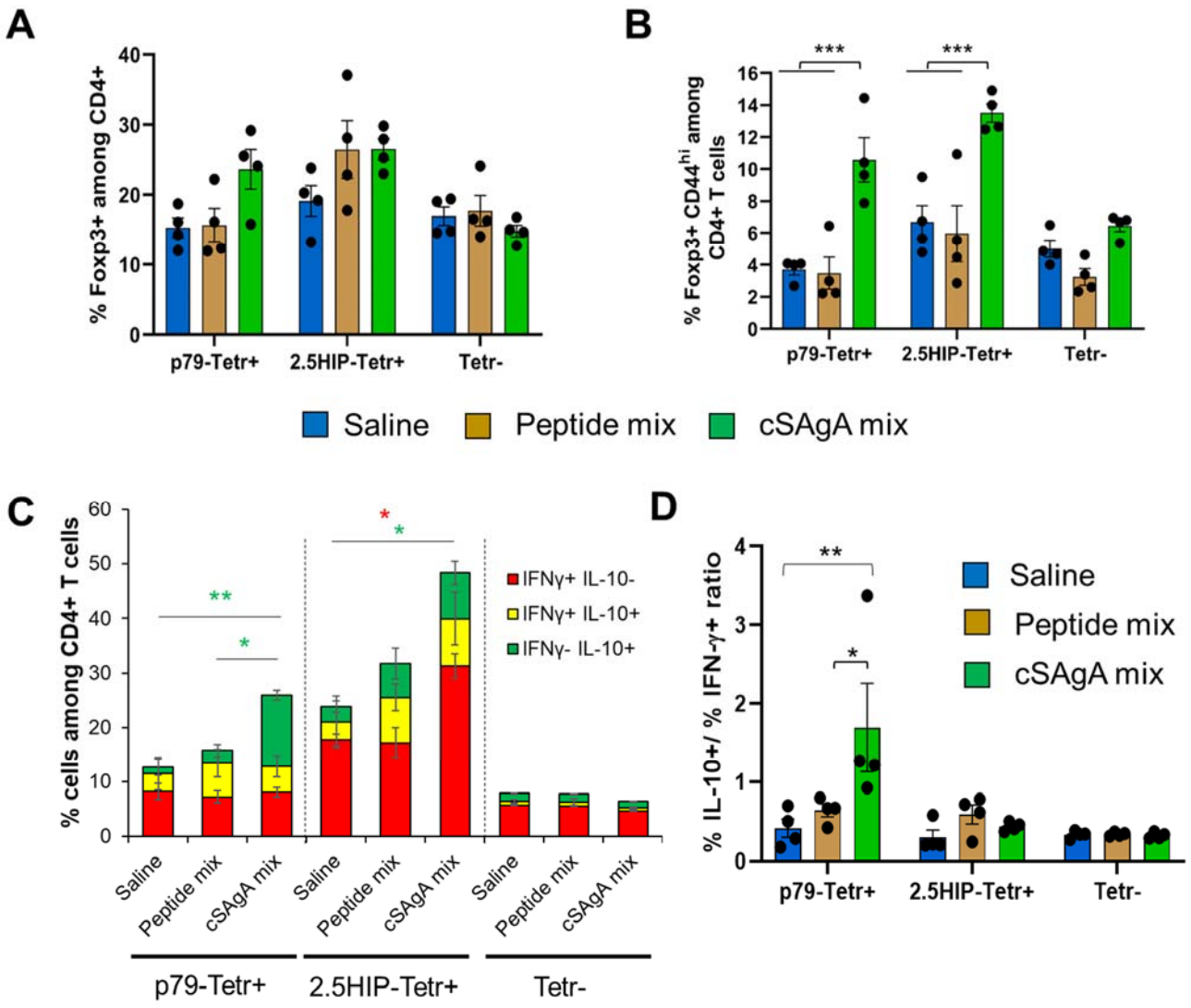

Figure S7. Responses of endogenous p79 and 2.5HIP-reactive CD4+ T cells to SAgAs versus free peptides. (**A**,**B**) Expression of Foxp3 on p79-Tetr+, 2.5HIP-Tetr+ and Tetr- CD4+ T cells, showing % of Foxp3+ (A) and of Foxp3+ CD44^{hi} (B). (**C,D**) Expression of IL-10 and IFNγ on p79-Tetr+, 2.5HIP-Tetr+ and Tetr- CD4+ T cells shown as % of IFNγ single positive, IL-10 single positive and IFNγ IL-10 double positive cells (C) and ratio of % IL-10+ / % IFNγ+ (D). All graphs show the mean ± SEM of 4 mice per group and data shown are from spleen. Statistical analysis was performed using two-way ANOVA/Tukey for all panels. In panel C, significant changes for IFNγ- IL-10+ populations are indicated with green stars and for IFNγ+ IL-10- populations with red stars.

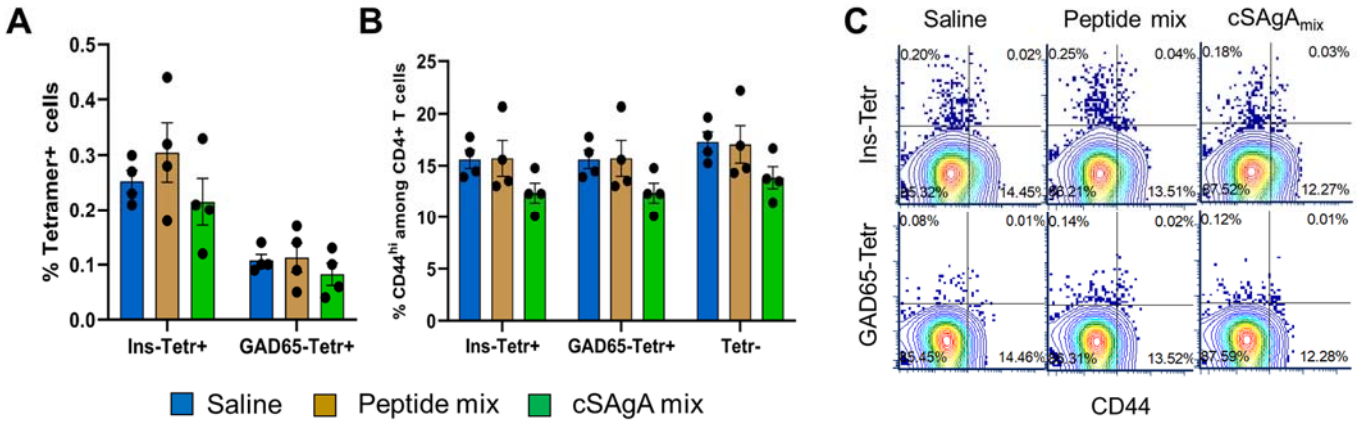

Figure S8. Frequency and activation status of endogenous CD4+ T cells reactive to InsB9-23 and GAD65(286-300) following treatment with free peptide mix or cSAgA mix (with p79 and 2.5HIP). Detection of Ins-Tetr+ and GAD65-Tetr+ T cells among CD4+ T cells (**A**), % $CD44^{hi}$ cells among Tetr+ and Tetr- CD4+ T cells (**B**) and representative dot plots (**C**). Graphs show the mean ± SEM of 4 mice per group and data shown are from spleen. Statistical analysis was performed using two-way ANOVA/Tukey.